The role of rheological heterogeneities in postseismic deformation

James D P Moore[1,2], Sambuddha Dhar[3], Jun Muto[3], Daisuke Sato[4], Youichiro Takada[5]
earth@jamesdpmoore.com
[1]Institute of Geophysics, SGEES, Victoria University of Wellington, Wellington, New Zealand
[2] Earth Observatory of Singapore, Nanyang Technological University, Singapore, [3] Tohoku University, Japan
[4] Kyoto University, Japan [5] Hokkaido University, Japan

Along-Arc Heterogeneous Rheology Inferred from Postseismic deformation of the 2011 Tohoku-oki Earthquake

The Japan forearc plays a crucial role in the postseismic deformation in response to the enormous stress perturbation induced by the 2011 Tohoku-oki earthquake. Dense geodetic observations (Fig 1) across Japan have revealed coupled interactions between afterslip on the plate interface and viscous deformation in the mantle wedge, and detailed numerical models can provide profound insights into its rheology. Recent studies revealed the pervasive presence of stagnant sections in the forearc mantle of the Tohoku subduction zone. However, further investigation is required to delineate the stagnant part of the mantle wedge (cold nose) and its associated along-arc variation over northeast Japan. Here we utilize the newly deployed geodetic network across Fukushima-Niigata and compare the surface deformation pattern to that of the Miyagi-Yamagata corridor close to the main rupture area.

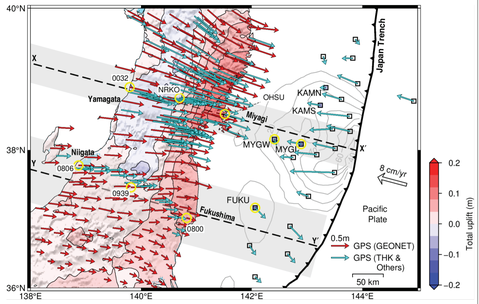

Map-view of observed postseismic displacement of the 2011 Tohoku-oki earthquake over NE Japan (September 2012-May 2016). The black-dashed lines (XX' and YY') and their shadow indicate trench-normal, two-dimensional transects and the corridors for projecting GNSS observations. The seafloor stations and coseismic slip distribution are represented by black-squares and grey contour lines (10 m intervals), respectively. The yellow circles correspond to sites 0032, NRKO, OHSU, MYGW, and MYGI for Miyagi corridor and sites 0806, 0939, 0800, and FUKU for Fukushima corridor.

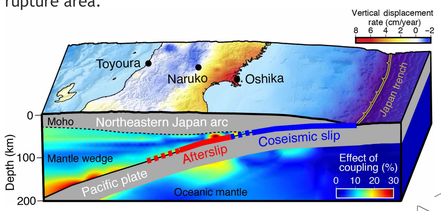

Schematic of mechanical coupling between viscoelastic relaxation and afterslip. Contours show the relative importance of mechanical coupling (%) on subsurface deformation after 6 years. The effect of coupling is calculated by the ratio of the difference in strain between the coupled and uncoupled models to the total strain in the mechanically coupled model. Coupling between viscoelastic flow and afterslip is the most important at the downdip of the mainshock below the coastline.

We present a three-dimensional rheological model using laboratory-derived constitutive laws to simulate geodetic observations including displacement fields and their time series in the Unicycle community code (Moore, Barbot, et. al. 2019).

Power law Burgers viscoelastic rheology:

$$\dot{\epsilon}_{\mathrm{M}} = A_{\mathrm{M}}\sigma^{n}C_{\mathrm{OH}}^{r}\exp\left(-\frac{Q+PV}{RT}\right)$$

$$\dot{\epsilon}_{\mathrm{K}} = A_{\mathrm{K}}(\sigma - 2G_{\mathrm{K}}\epsilon_{\mathrm{K}})^{m}C_{\mathrm{OH}}^{r}\exp\left(-\frac{Q+PV}{RT}\right)$$

Velocity strengthening afterslip: $v = 2v_0\sinh\left(\frac{\Delta\tau}{(a-b)\sigma_n}\right)$

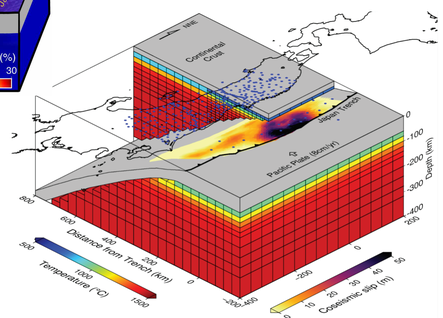

Model framework with temperature distribution in viscoelastic structure. The cross-section shown in the mantle wedge corresponds to the Miyagi transect. The grey area represents elastic structure.

Along-arc hetereogeneity

Our results suggest along-arc heterogeneity in the forearc mantle rheology, specifically we find a narrower cold nose in the Miyagi region and a wider one for the Fukushima forearc. We also image the volcanic front, particularly around Mt Naruko and **Mt Kurikoma**. The geodetic inferences on the forearc variation are consistent with spatial heterogeneity in the cutoff depth for shallow earthquakes as well as the geothermal gradient between the Miyagi and Fukushima regions.

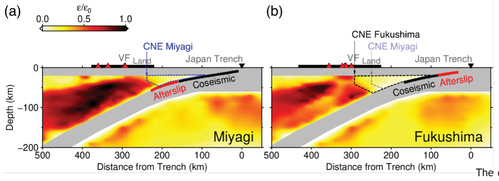

The normalized total strain for (a) the Miyagi and (b) the Fukushima transect. Total strain is given by viscous strain ε divided by coseismic strain ε0 over 5.2 years. The grey area indicates elastic oceanic mantle and continental crust. The location of large coseismic slip (≥ 10 m) and accumulated afterslip (≥ 1 m) over 5.2 years are marked in black and red colors, respectively. CNE and VF stands for cold-nose edge and volcanic front, respectively.

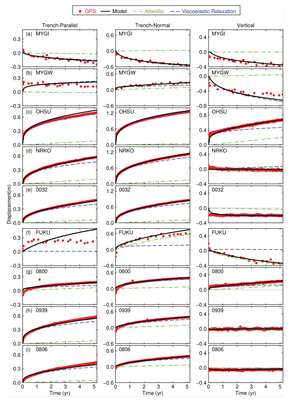

The observed and modeled displacements (left: trench-parallel component, middle: trench-normal component, right: vertical component) for the stations MYGI (a), MYGW (b), OHSU (c), NRKO (d), 0032 (e), FUKU (f), 0800 (g), 0939 (h) and 0806 (i) along Miyagi and Fukushima corridors over 5.2 years. Black lines, green and blue dashed lines represent modelled displacements and displacements by afterslip and viscoelastic relaxation, respectively.

Iwate-Miyagi Nairiku (Mw 6.8, 2008)

The Iwate-Miyagi Nairiku Earthquake (hereafter IMNE) occurred on June 14, 2008 (Mj 7.2) at the eastern flank of Mt. Kurikoma, an active volcano. The IMNE is characterized by conjugate fault rupture: west-dipping and east-dipping faults brought about complex surface deformation (e.g., Takada et al., 2009). A relatively large amount of post-seismic deformation has been observed by GNSS surveys (e.g., Ohzono et al., 2012) and InSAR analyses. The post-seismic displacement field at high spatial resolution detected by InSAR should reflect multi-scale crustal heterogeneities in the hypocentral area.

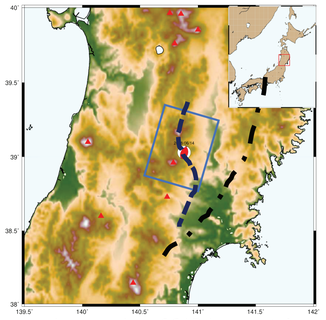

In this study we include an InSAR time-series analysis to identify the post-seismic displacements in the hypocentral area using a series of SAR images taken by ALOS from descending orbit. In the 2.2 years after IMNE, we detected the following signals: (1) LOS length increase at the footwall of the west-dipping fault, (2) LOS shortening at the hanging wall of the east-dipping fault, and (3) LOS shortening to the west of Mt. Kurikoma. We also found that these three signals accumulate with time. We interpret the first and the second signals due to afterslip on the west- and the east-dipping faults, respectively. The third signal reaches more than 10 cm in ~2 years, which indicates the existence of rheological heterogeneity to the west of **Mt. Kurikoma**. Interestingly, the location of the third signal coincides with the area of localized subsidence triggered by the 2011 Tohoku-Oki Earthquake (left column).

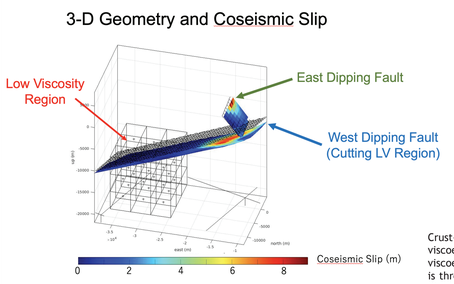

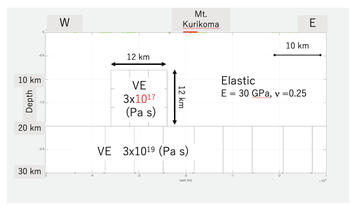

Crust-mantle structure with an elastic layer of 20 km thickness overlying a Maxwell viscoelastic substratum following Ohzono et al. (2012). Next, we put a localized viscoelastic volume at 8-20 km depth to the west of Mt. Kurikoma where the viscosity is three times lower than that of the substratum. Note the conjugate east and west dipping faults (left).

We construct a physical model of the postseismic deformation following IMNE using the integral method (Unicycle) and we consider fault slip, viscoelastic flow, intersecting conjugate faults (which requires very careful numerical treatment), and their interactions. We utilise the same governing equations as presented for Tohoku (left) and drive the model with the coseismic slip distribution as proposed by Iinuma et al. (2009). Our numerical results indicate that the postseismic slip on the west-dipping fault expands to the shallower and the deeper portion of the coseismic rupture area with time. Furthermore, the deeper extension of the postseismic slip reaches the low viscosity region to the west of Mt. Kurikoma, and it causes volumetric flow which strongly enhances surface uplift to the west of Mt. Kurikoma and explains LOS shortening there.

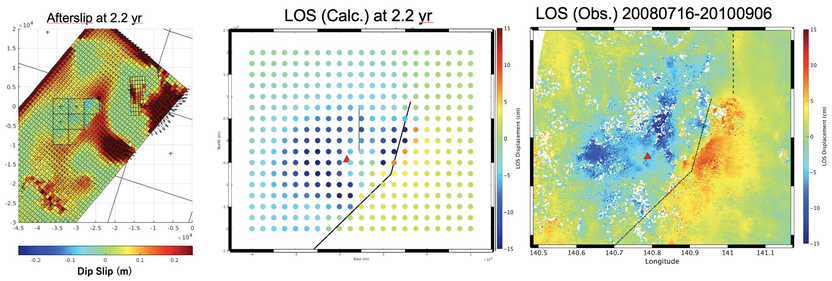

Left: cumulative afterslip at 2.2 years after the IMNE. Note the intersecting conjugate faults in the north-east and low viscosity region in the mid-west. The stress relaxation due to the low-viscosity region negates the need for any afterslip here. **Middle**: Line of sight modelled deformation. **Right**: Line of sight observed deformation.

Crucially, both studies - the postseismic deformation from Tohoku 2011 and Iwate-Miyagi 2008 image the same volcanic complex, at the same location, with similar viscoelastic properties, despite different driving earthquakes!

Displacements and stress associated with localised and distributed inelastic deformation with piecewise-constant elastic variations

We present a semianalytical method and expressions for computing the displacements, strains and stress due to localised (e.g. faulting) and distributed (volumetric) inelastic deformation in heterogeneous elastic full- and half-spaces. Variations in elastic properties are treated as piecewise-constant homogeneous subregions as in orthodox multiregion approaches. The deformation in the subregions is solved by matching the interface traction and displacement conditions for contrasting elastic parameters. We show equivalence between the integral equation convolving boundary traction and those convolving displacement discontinuities and volumetric inelastic strain in the representation theorem for a bounded volume. This equivalence allows us to express the deformation fields in the half-/full- space which comprises those subregions by using virtual fault displacement elements or volumetric eigenstrain elements, the integral kernels of which have known analytic forms for finite sources in homogeneous volumes.

Dual Equivalent Inclusion

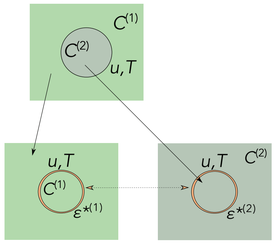

Schematic of the dual equivalent inclusion method. The problem to be solved concerns a medium made of subdomains (dark and light greens in the panel) of different elastic properties, the interfaces of which satisfy the displacement (u) continuity and the traction (T) balance. Facing domains are solved with conjugate inclusions involving the thin layers of the eigenstrains ε (orange in the panel) that deal with the boundary conditions of the interface.

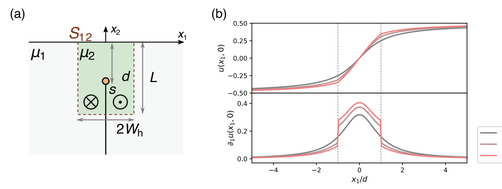

Example of a anti-plane strike slip fault with fault tip inside a compliant zone. (a) The crack tip is buried at a depth, d, below the surface within a compliant zone of dimensions L by W_h. The x_1 axis is parallel to the ground surface, and the x_2 axis lies vertically along the fault. (b) Computed surface deformation (displacement u and along-surface displacement gradient $\partial_1 u$). The deformation fields are computed for three different relative rigidities where $\gamma=\mu_1/\mu_2$ for $W_h=L/2-d$ with normalisation s=d=1. The location of the material interface on the ground surface is shown by grey dashed lines.

Schematic of the 3-D example. A rectangular transverse fault (orange face) of horizontal dimension L_F by W_F slips uniformly by s and intersects the surface (grey plane). The outcropping cuboidal compliant zone V_2 (green volume) of equal dimensions $L_F(>W_F)S$ encloses a crack tip and is embedded in a stiffer (half-space) volume V_1. The interface S_{12} of the subvolumes is mirror-symmetric with regard to the along-strike and along-normal directions of the fault. A right-handed coordinate for the half-space $x_3<0$ is defined such that x_1 and x_3 axes are aligned with the horizontal and vertical sides of the fault, respectively. It further sets the x_2 axis, such that the along-strike component of the displacement vector takes the same sign as that of s at $x_2=+0$ on the fault.

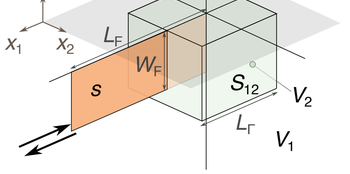

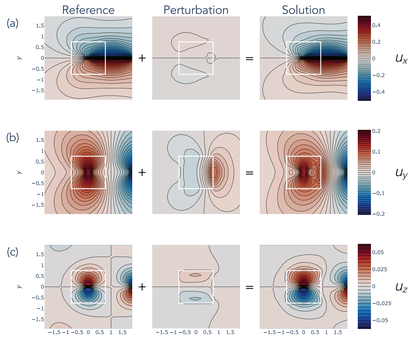

Surface displacements, (a) u_1, (b) u_2 and (c) u_3, in the 3-D example of a cuboid compliant zone. We have decomposed the deformation into the reference homogenous model, the pertubation due to the inclusion of the compliant zone, and the total deformation field for the heterogeneous model. The parameters are set at $L_F/2=W_F=2L_r/3$, $\mu_1/\mu_2=3$ and s=-1. The coordinate values are normalised by W_F. Coordinate axes x_1 and x_2 are expressed for brevity as x and y, respectively. The white solid lines show the location of the material interface on the ground surface.

The horizontal surface deformation projected onto a simulated line of sight (LOS) direction, visualised in a manner similar to the interferometric synthetic aperture radar. The simulated LOS direction is indicated by the arrows and parametrised by its compass bearing from North (the y-axis). We simulate three LOS angles for 80°, 45° and 20° in panels (a), (b) and (c), respectively. The fringes represent the deformation values modulo the characteristic wavelength of the measurements, the value of which is set at 0.17 in the figure. The parameter values and unit sets are the same as above, and we compare the Heterogeneous Model to a reference Homogeneous Model, and their residual.

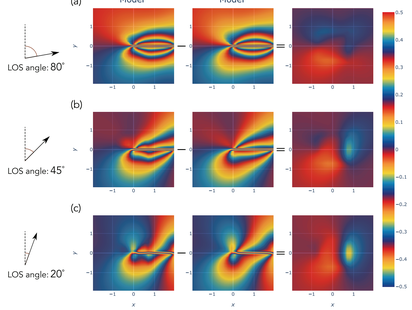

Our work allows users to model heterogeneous geological structures, with a number of primary geophysical applications, including earthquake and volcano deformation, where variations in elastic parameters may present a substantial contribution to the observed deformation. We shall incorporate this theoretical advance into our work looking at the Japan arc (left and centre columns), and the code will be available for general modelling in a new Unicycle release later in 2022.

For more about the Tohoku postseismic please see:
Muto J, Moore J D P, Barbot S, Iinuma T, Ohta Y, Horiuchi S, Hikaru I. Coupled afterslip and transient mantle flow after the 2011 Tohoku earthquake. [2019, Science Advances] https://www.science.org/doi/10.1126/sciadv.aaw1164

Sambuddha Dhar, Jun Muto, Yoshiaki Ito, Satoshi Miura, James D P Moore, Yusaku Ohta, Takeshi Iinuma, Along-arc heterogeneous rheology inferred from post-seismic deformation of the 2011 Tohoku-oki earthquake, Geophysical Journal International, Volume 230, Issue 1, July 2022, Pages 202–215, https://doi.org/10.1093/gji/ggac063

For more about Elastic Heterogeneity please see:
Dye S K Sato, James D P Moore, Displacements and stress associated with localized and distributed inelastic deformation with piecewise-constant elastic variations, Geophysical Journal International, Volume 229, Issue 3, June 2022, Pages 1990–2032, https://doi.org/10.1093/gji/ggac046

Unicycle Community Code: *Muto et. al.:* *Dhar et. al.:* *Sato et. al.:*

James D P Moore, Sylvain Barbot, Lujia Feng, Yu Hang, Valere Lambert, Eric Lindsey, Sagar Masuti, Takanori Matsuzawa, Jun Muto, Priyamvada Nanjundiah, Rino Salman, Sharadha Sathiakumar, & Harpreet Sethi. (2019). jdpmoore/unicycle: Unicycle. In Coupled afterslip and transient mantle flow after the 2011 Tohoku earthquake, Science Advances 2019 (1.1, Vol. 5, Number 9). Zenodo. https://doi.org/10.5281/zenodo.5688288

Muto J, Moore J D P, Barbot S, Iinuma T, Ohta Y, Horiuchi S, Hikaru I. Coupled afterslip and transient mantle flow after the 2011 Tohoku earthquake. [2019, Science Advances] https://www.science.org/doi/10.1126/sciadv.aaw1164

S. Barbot, J. D. P. Moore, V. Lambert, Displacement and stress associated with distributed anelastic deformation in a half-space. Bull. Seismol. Soc. Am. 107, 821–855 (2017).

V. Lambert, S. Barbot, Contribution of viscoelastic flow in earthquake cycles within the lithosphere-asthenosphere system. Geophys. Res. Lett. 43, 10142–10154 (2016).

Barbot, S., Fialko, Y. & Bock, Y., 2009. Postseismic deformation due to the Mw 6.0 2004 Parkfield earthquake: Stress-driven creep on a fault with spatially variable rate-and-state friction parameters, J. Geophys. Res. Solid Earth, 114.